

~~CONFIDENTIAL~~

~~53-34-80~~



TECH LIBRARY KAFB, NM  
0143829

# RESEARCH MEMORANDUM

SOME EFFECTS OF AEROELASTICITY AT MACH NUMBERS  
FROM 0.7 TO 1.6 ON THE ROLLING EFFECTIVENESS OF THIN  
FLAT-PLATE DELTA WINGS HAVING 45° SWEEP LEADING EDGES  
AND FULL-SPAN CONSTANT-CHORD AILERONS

By Edward T. Marley and Roland D. English

Langley Aeronautical Laboratory  
Langley Field, Va.

*Unclassified*  
*NACA Tech Rep Aeronautics #111*  
*(to be changed to CHANGE)*

*28 Jan 57*

*MS*

*[Handwritten signature]*

Grant (to be changed to CHANGE)

*4 Apr 61*

CLASSIFIED DOCUMENT

~~Information reported herein is the property of the National Aeronautics and Space Administration and is to be controlled in accordance with the provisions of the Federal Acquisition Regulation (FAR) 27.114, the transmission or revelation of which in any form to an unauthorized person is prohibited by law.~~

## NATIONAL ADVISORY COMMITTEE FOR AERONAUTICS

WASHINGTON

February 19, 1952

~~CONFIDENTIAL~~

*319.98/13*

7303

NACA RM L51L05

~~CONFIDENTIAL~~

## NATIONAL ADVISORY COMMITTEE FOR AERONAUTICS

## RESEARCH MEMORANDUM

SOME EFFECTS OF AEROELASTICITY AT MACH NUMBERS  
FROM 0.7 TO 1.6 ON THE ROLLING EFFECTIVENESS OF THIN  
FLAT-PLATE DELTA WINGS HAVING  $45^\circ$  SWEPT LEADING EDGES  
AND FULL-SPAN CONSTANT-CHORD AILERONS

By Edward T. Marley and Roland D. English

## SUMMARY

The aeroelastic effects on wing-aileron rolling effectiveness and drag of thin flat-plate delta wings with  $45^\circ$  swept leading edges and plain constant-chord ailerons have been investigated. This investigation has been carried out over a Mach number range of 0.7 to 1.6 by means of rocket-propelled test vehicles in free flight. The results show a near-linear decrease in lateral control effectiveness with a decrease in the wing torsional stiffness. An aileron-effectiveness reversal was experienced with the more flexible delta-wing models.

## INTRODUCTION

In the course of a continuing program by the Langley Pilotless Aircraft Research Division to determine the effects of aeroelasticity upon some of the most promising wing-control configurations for high-speed flight, an investigation was conducted by using simplified models to determine the fundamental aeroelastic characteristics of flap-type controls on delta wings. Because of the laborious methods now involved in predicting aeroelastic effects on delta wings, these data are presented without analysis or comparison with theory in order to make them immediately available to designers. The trends observed from these data should be applicable to many delta-wing aircraft and missile designs.

~~CONFIDENTIAL~~

## SYMBOLS

b	diameter of circle swept by wing tips (with regard to rolling characteristics, this diameter is considered to be the effective span of the three-fin models, see fig. 2), feet
P	rolling velocity, radians per second
V	flight-path velocity, feet per second
pb/2V	wing-tip helix angle, radians
C <sub>DT</sub>	total drag coefficient based on exposed area of three wing panels
R	Reynolds number based on a wing chord of 0.521 foot
δ <sub>a</sub>	deflection of each aileron in a plane perpendicular to aileron hinge line, degrees
P	concentrated load applied on 17-percent-chord line at 0.88b/2
δ	bending deflection of test wing along 17-percent-chord line under load P, inches
q	dynamic pressure, pounds per square foot
m	concentrated couple applied on wing at 0.86b/2 in a plane perpendicular to wing-chord plane and parallel to model center line, inch-pounds
θ	angle of twist in plane of m due to m, radians
θ/m	wing torsional-stiffness parameter, radians per inch-pound
δ/p	wing bending-stiffness parameter, inches per pound
y	distance to 17-percent-chord line measured perpendicular from model center line, feet

## MODELS AND TECHNIQUES

The general arrangement of the models used in this investigation is shown in the photograph which is presented as figure 1 and in the sketches presented as figures 2 and 3.

Each model had three flat-plate delta wings with 45° swept leading edges. The aspect ratio for all models was 4; other model information is as follows:

Model	$\delta_a$	Wing material	Average wing thickness, in.
1	2.87	Solid steel	0.125
2	2.72	Solid aluminum	.125
3	2.56	Solid aluminum	.125
4	2.36	Solid magnesium	.122
5	2.50	Solid magnesium	.122

The wing material was varied in order to determine the effects of wing flexibility on the aileron rolling effectiveness. Each of the test vehicles had constant-chord plain trailing-edge ailerons obtained by beveling the aft section of the wing (see sketch in fig. 3).

These test vehicles were propelled by a two-stage rocket-propulsion system to a Mach number of about 1.6. Time histories of the rolling velocity obtained by special spinsonde radio equipment and flight-path velocity obtained by Doppler radar were recorded during a 12-second period of coasting flight following sustainer-rocket burnout. These data, together with atmospheric data obtained by radiosonde measurements, provided information for the computation of the rolling-effectiveness parameter  $pb/2V$  and the total drag coefficient  $C_{DT}$  as functions of Mach number. Detailed descriptions of the flight testing technique can be found in references 1 and 2. The range and variation of Reynolds number with Mach number for the models flown are shown in figure 4.

ACCURACY

The wing torsional-stiffness parameter  $\theta/m$  was accurate to within  $\pm 5$  percent. The experimental error is estimated to be within the following limits:

	Subsonic	Supersonic
$pb/2V$ . . . . .	$\pm 0.004$	$\pm 0.003$
$C_{DT}$ . . . . .	$\pm 0.005$	$\pm 0.005$
$M$ . . . . .	$\pm 0.005$	$\pm 0.005$

The sensitivity of the experimental technique is such that much smaller irregularities in the variation of  $pb/2V$  with Mach number may be detected.

## RESULTS AND DISCUSSION

The variation of the rolling-effectiveness parameter per degree of aileron deflection  $(pb/2V)/\delta_a$  with Mach number for each of the models tested is presented in figure 5. The corresponding values of the dynamic pressure are shown in figure 6. Figure 7 presents cross plots of  $(pb/2V)/\delta_a$  against wing torsional stiffness.

The results of structural tests made on the models are presented in figure 8 wherein the variation of the flexural and torsional characteristics is shown as plots of  $\delta/p$  and  $\theta/m$  as functions of the non-dimensional span station  $y/(b/2)$ . It is noted that the recorded deflection in bending  $\delta/p$  for similar wings of different material is not inversely proportional to the material modulus as would be expected, a probable explanation being that the root mount distorted and caused the wing to rotate about its root which was not compensated for in the curve in figure 8.

Figure 5 shows clearly the effect of wing flexibility on the rolling effectiveness of these delta-wing models. The more rigid steel wing model had the highest values of  $(pb/2V)/\delta_a$  throughout the Mach number range; lower values were obtained for the more flexible aluminum wing models; and the magnesium wing models, which had the most flexible wings, had the lowest values of  $(pb/2V)/\delta_a$ . An aileron-effectiveness reversal occurred for the magnesium and aluminum wing models at Mach numbers of about  $M = 0.98$  and  $M = 1.2$ , respectively.

The cross plots of figure 7 show the delta wings of this investigation to have a near-linear decrease in rolling effectiveness with a decrease in wing torsional stiffness; this result is in keeping with the predictions of reference 3 for more conventional wing plan forms.

The rigid-wing values presented in figure 5 of this paper were obtained by extrapolation from cross plots of  $pb/2V$  against wing torsional stiffness. This extrapolation was justifiable since the values of  $q$  at any given Mach number for all of the models were essentially the same; therefore, the wing torsional stiffness remains as the primary variable producing a deviation from the rigid-wing rolling effectiveness of otherwise similar models.

Figure 9 presents the total drag coefficient against Mach number for the models of the present investigation along with the estimated supersonic body drag coefficients for these models.

#### CONCLUSIONS

Wing-aileron rolling effectiveness was obtained over a Mach number range from 0.7 to 1.6 for thin flat-plate delta wings. From these data the following conclusions are drawn:

1. The effects of aeroelasticity upon delta wings are similar to those previously experienced with more conventional plan forms; that is, the control effectiveness had a near-linear decrease with a decrease in wing torsional stiffness.
2. Aileron-effectiveness reversal was experienced for the more flexible wing models of this investigation.

Langley Aeronautical Laboratory  
National Advisory Committee for Aeronautics  
Langley Field, Va.

#### REFERENCES

1. Sandahl, Carl A., and Marino, Alfred A.: Free-Flight Investigation of Control Effectiveness of Full-Span 0.2-Chord Plain Ailerons at High Subsonic, Transonic, and Supersonic Speeds to Determine Some Effects of Section Thickness and Wing Sweepback. NACA RM L7D02, 1947.
2. Pitkin, Marvin, Gardner, William N., and Curfman, Howard J., Jr.: Results of Preliminary Flight Investigation of Aerodynamic Characteristics of the NACA Two-Stage Supersonic Research Model RM-1 Stabilized in Roll at Transonic and Supersonic Velocities. NACA RM L6J23, 1947.
3. Pearson, Henry A., and Aiken, William S., Jr.: Charts for the Determination of Wing Torsional Stiffness Required for Specified Rolling Characteristics or Aileron Reversal Speed. NACA Rep. 799, 1944. (Formerly NACA ACR L4L13.)

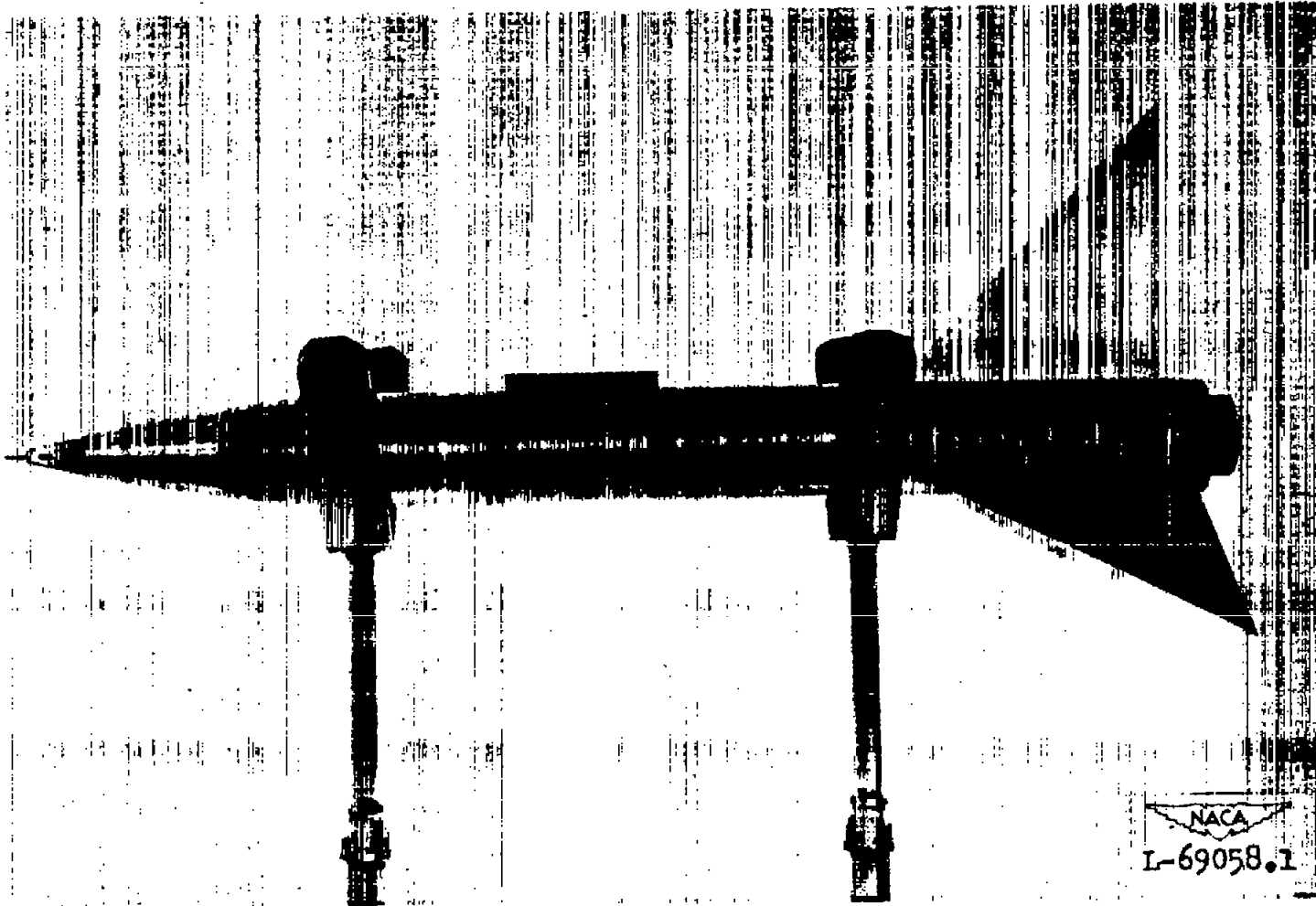


Figure 1.- Typical test model.

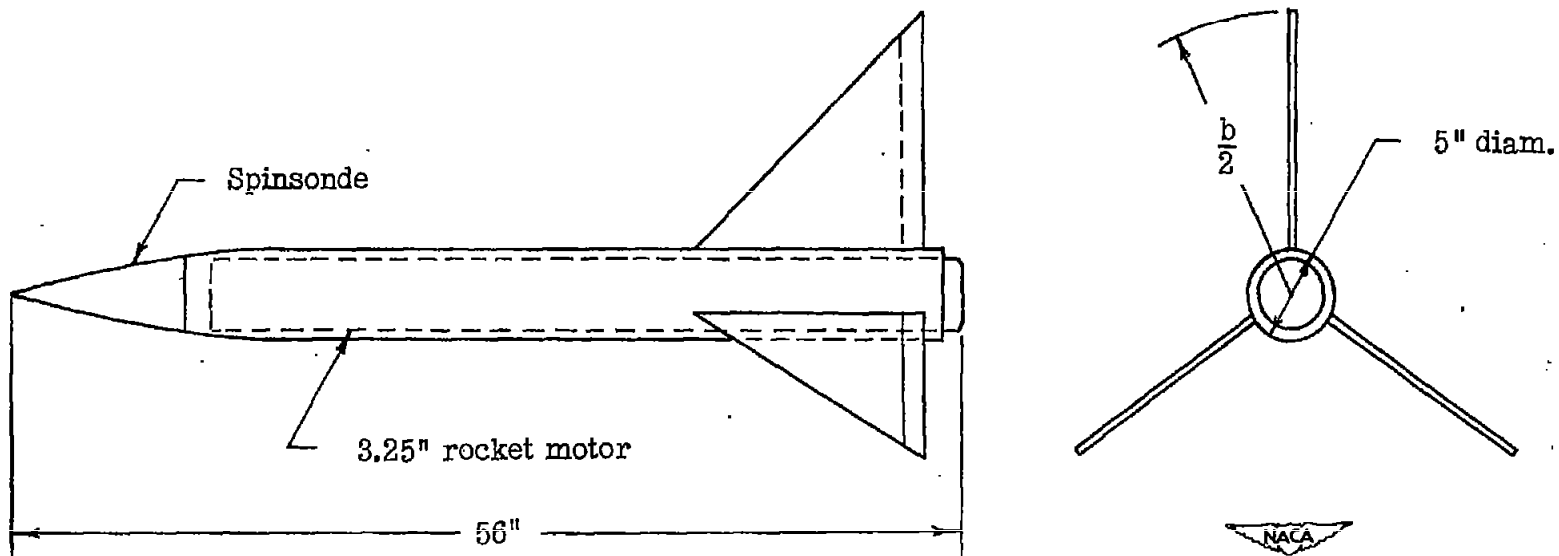


Figure 2.- General arrangement of test models.

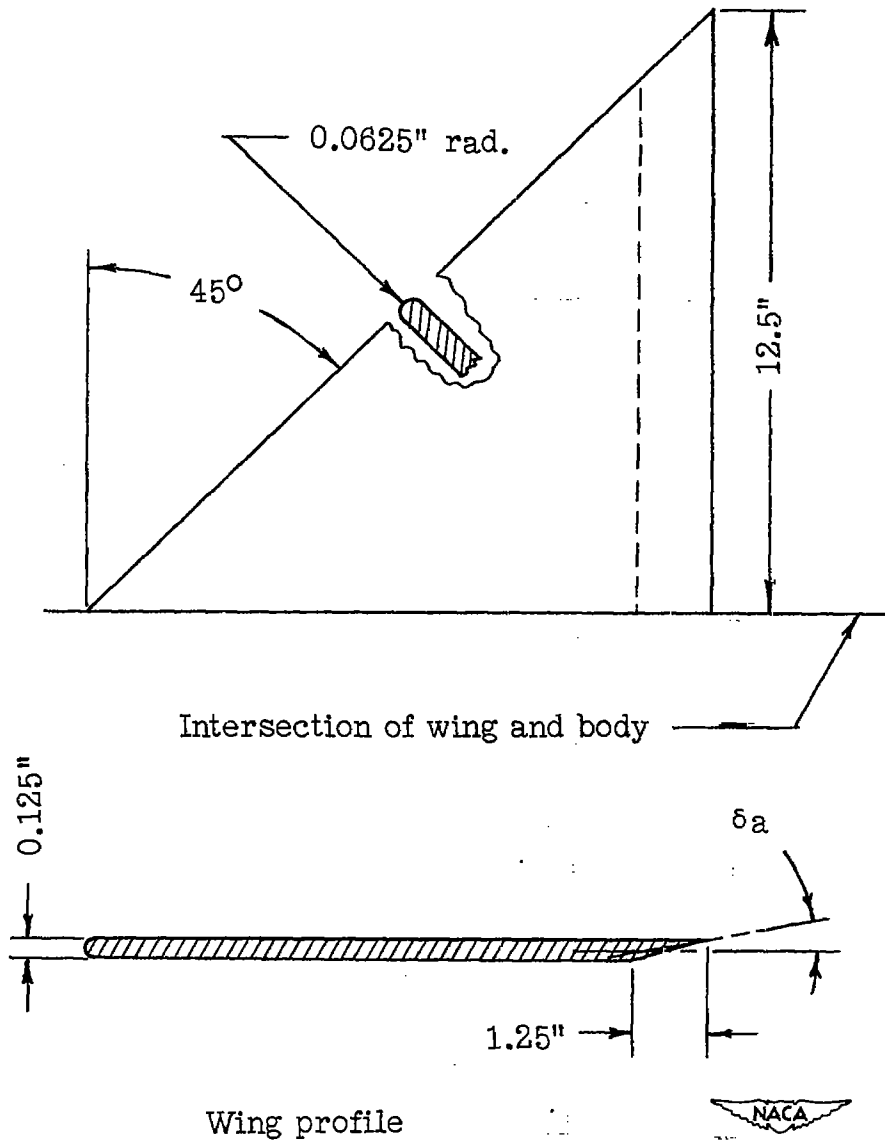
~~CONFIDENTIAL~~

Figure 3.- Plan form and section of test wings.

~~CONFIDENTIAL~~

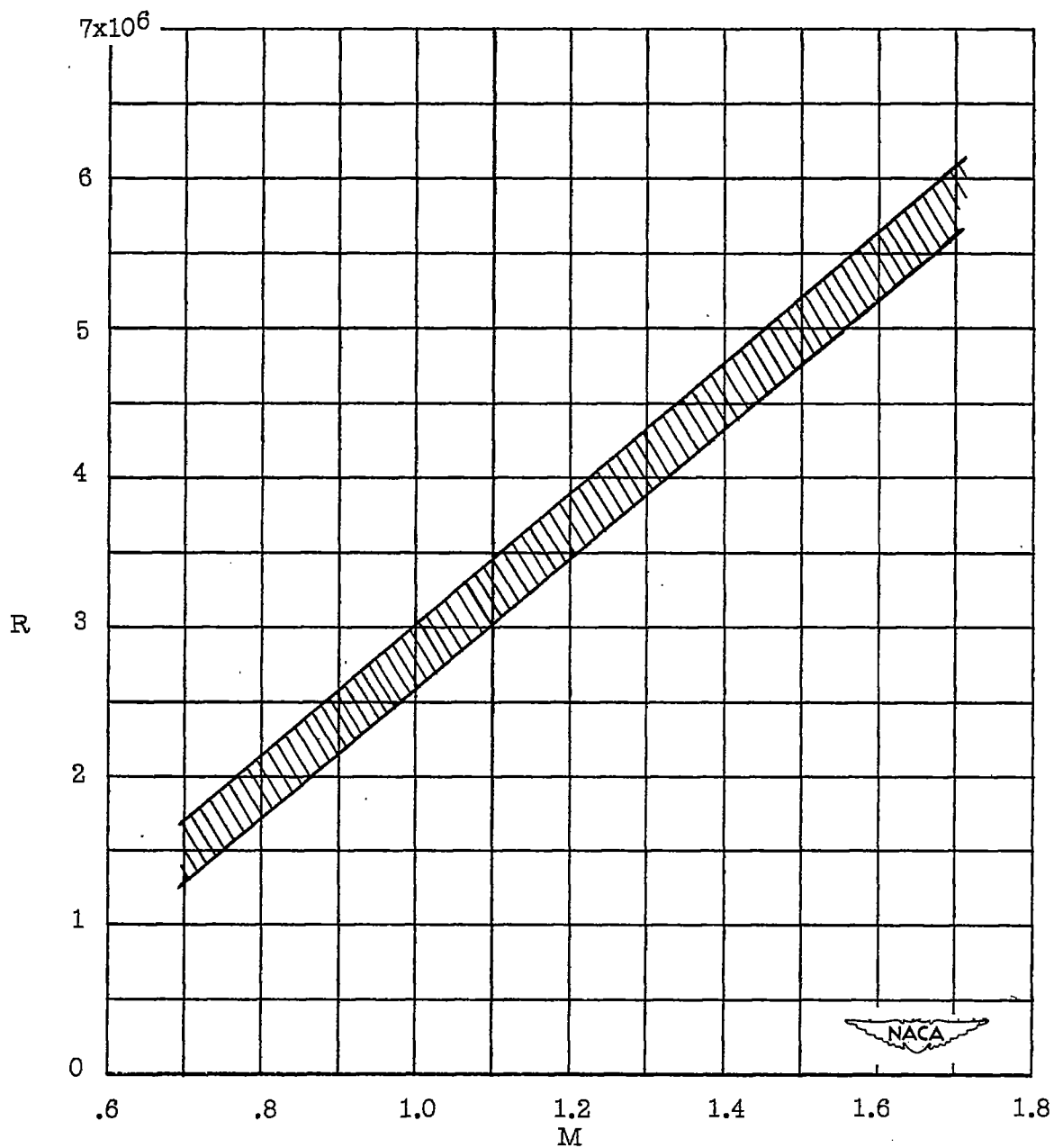


Figure 4.- Range and variation of Reynolds number with Mach number.  
Reynolds numbers based on a mean exposed chord of 0.521 foot.

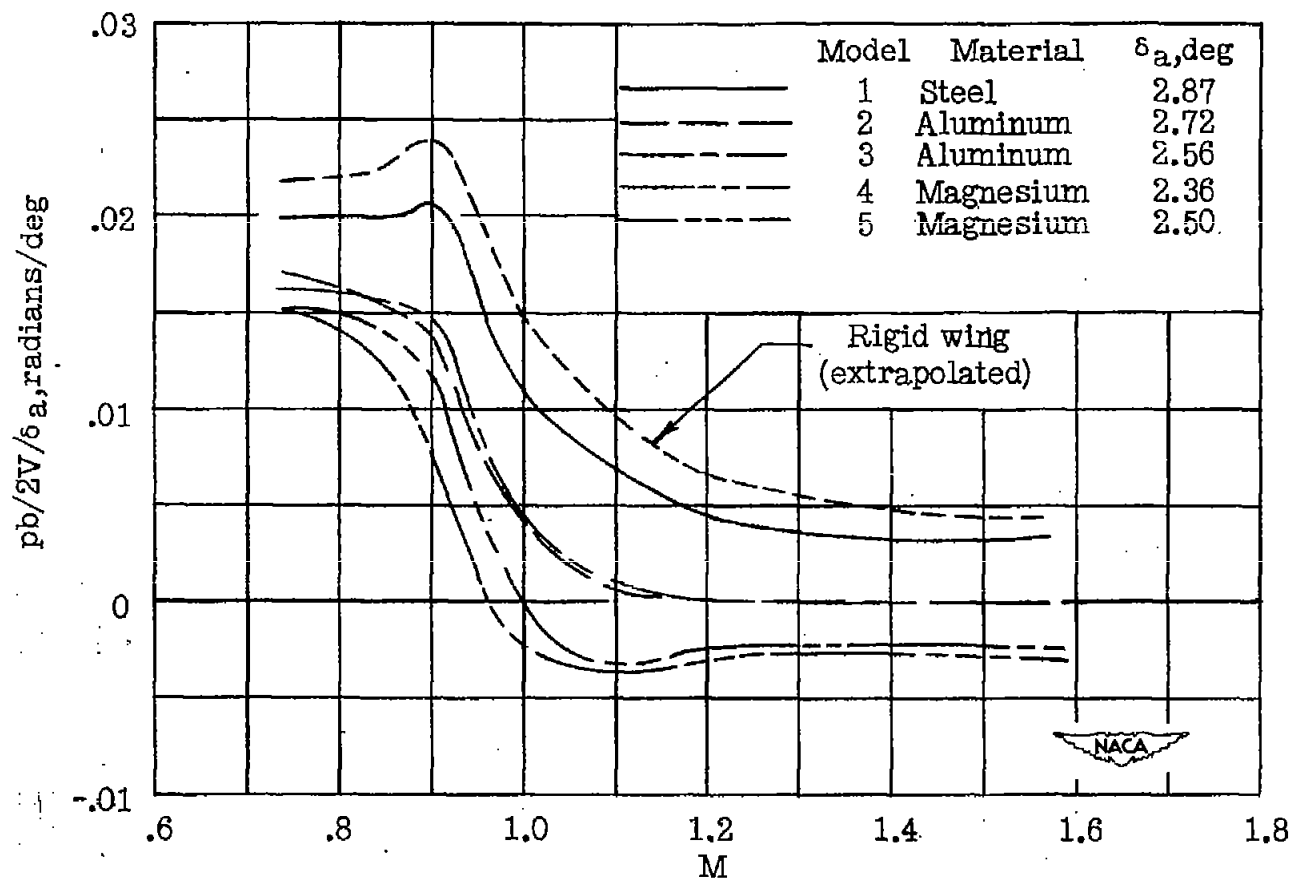


Figure 5.- Variation of rolling effectiveness per degree of flap deflection with Mach number.

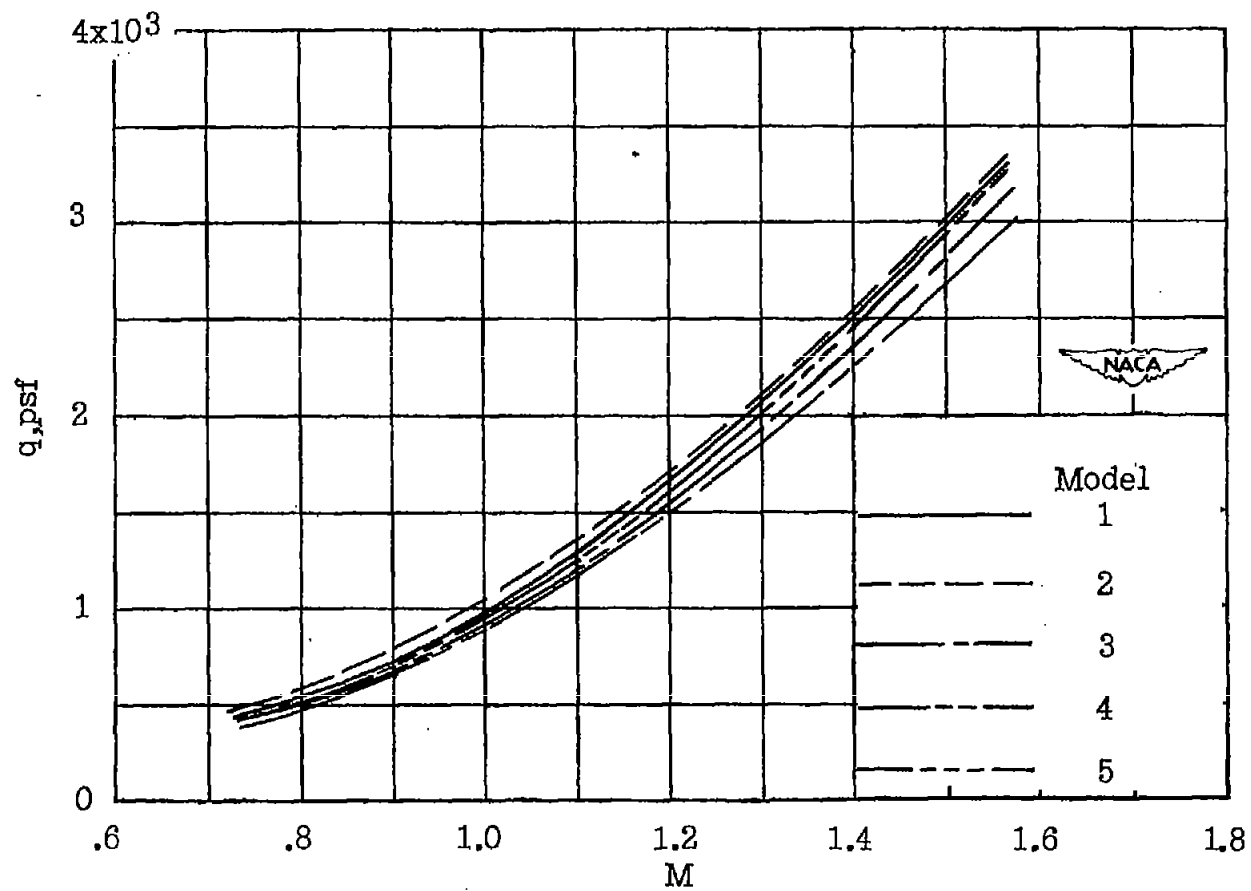


Figure 6.- Dynamic pressure  $q$  plotted against Mach number.

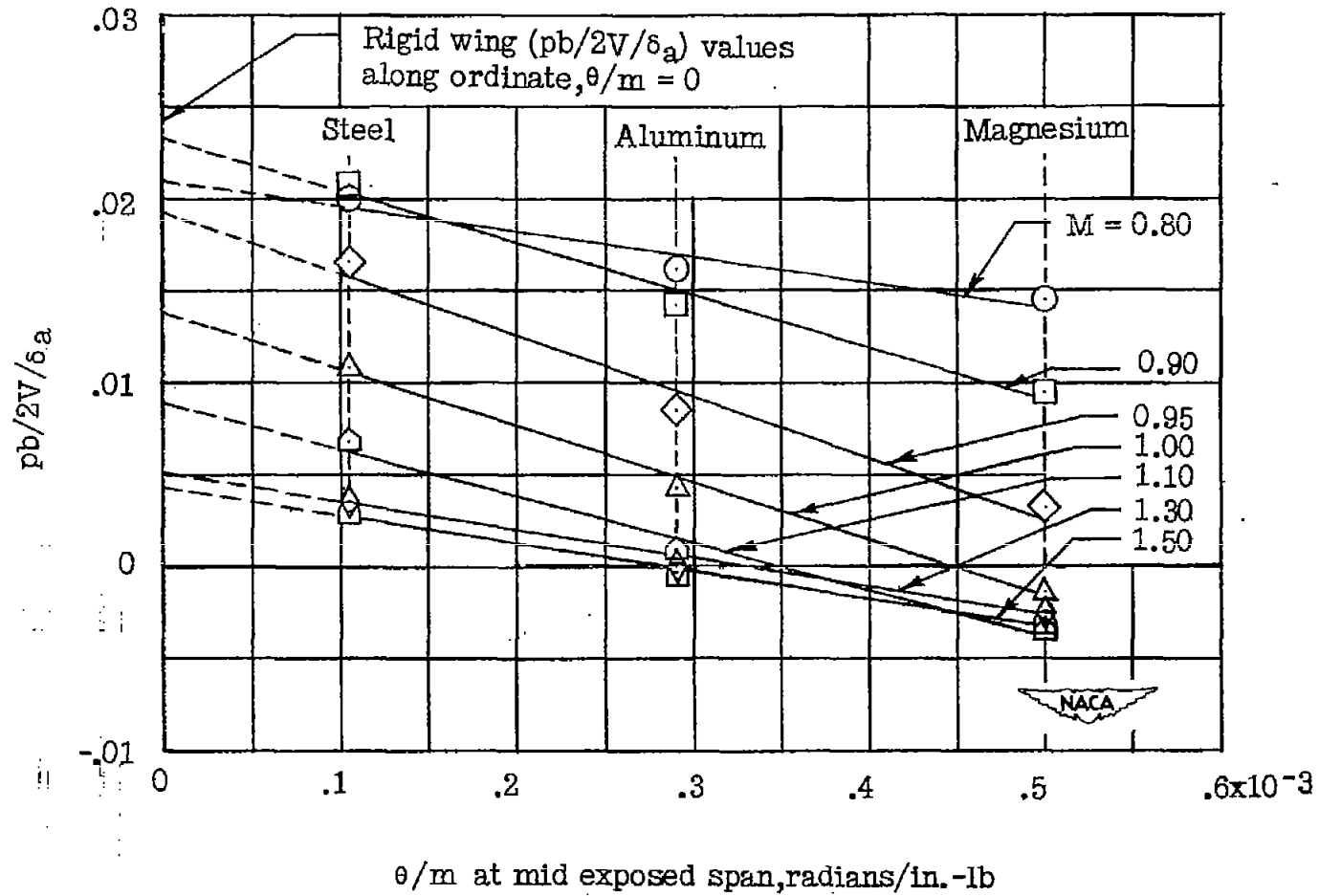


Figure 7.- Cross plot of  $pb/2V/\delta_a$  against  $\theta/m$  at mid exposed span.

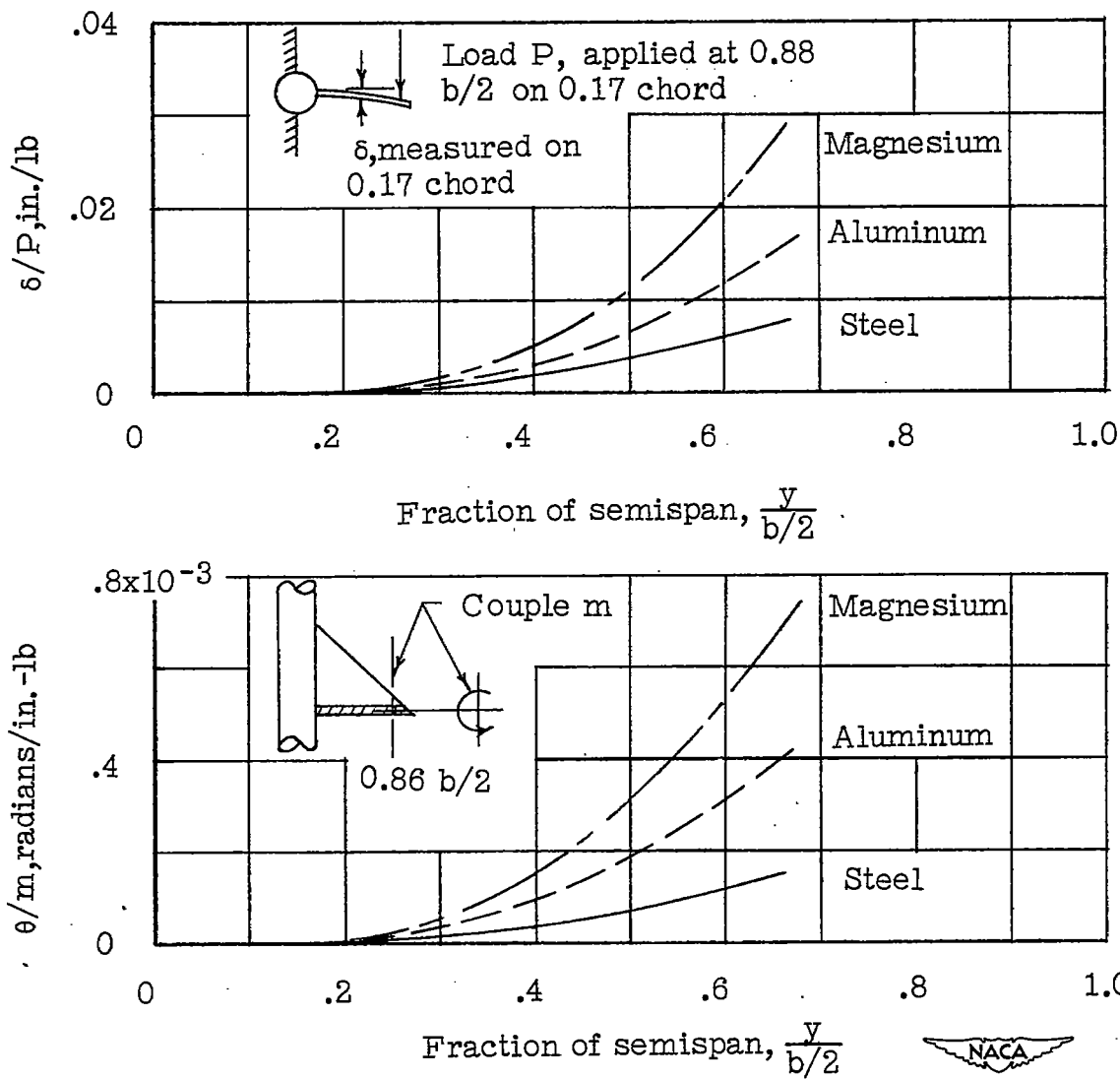


Figure 8.- Spanwise variation of torsional-stiffness parameter  $\theta/m$  and flexural-stiffness parameter  $\delta/P$ .

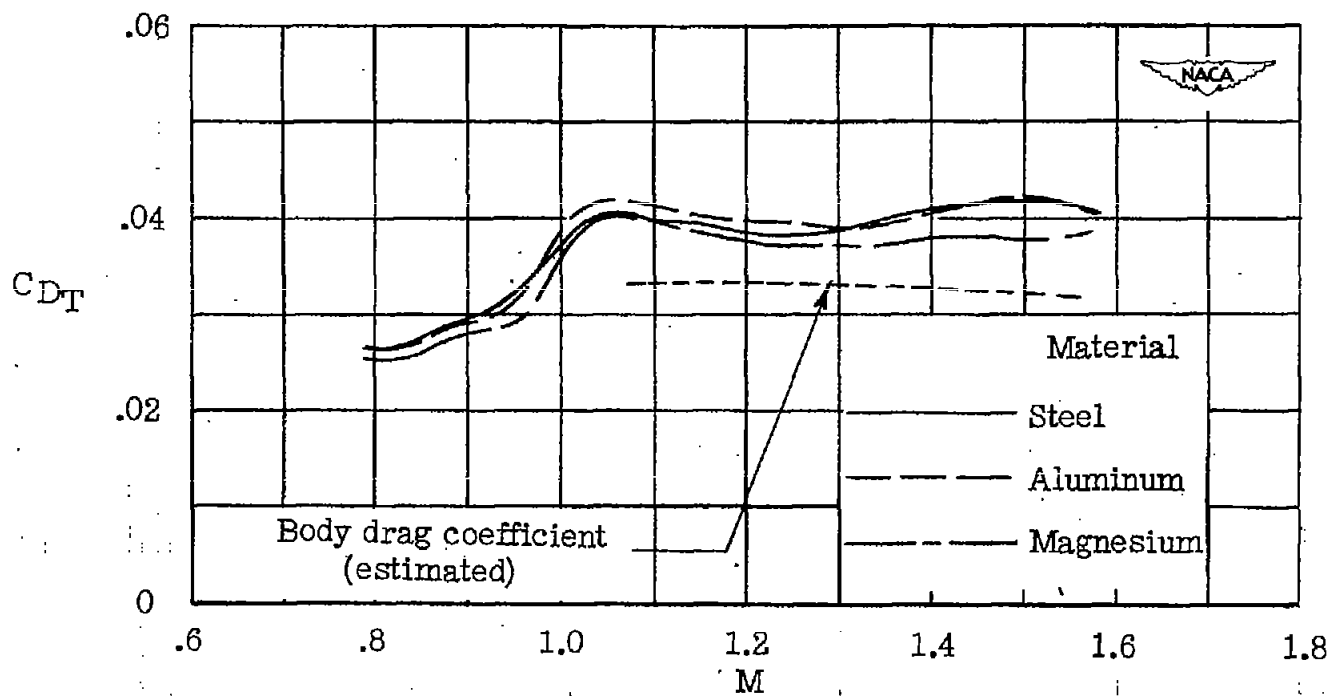


Figure 9.- Variation of total drag coefficient with Mach number.